IAC-13-C1.4.3

ORBIT CONTROL OF ASTEROIDS IN LIBRATION POINT ORBITS FOR RESOURCE EXPLOITATION

Matteo Ceriotti
School of Engineering, University of Glasgow, Glasgow, United Kingdom
matteo.ceriotti@glasgow.ac.uk

Joan Pau Sanchez Cuartielles
Department of Applied Mathematics I, Universitat Politècnica de Catalunya, Barcelona, Spain
jpau.sanchez@upc.edu

The fascinating idea of shepherding asteroids for science and resource utilisation is being considered as a very credible concept in a not too distant future. Past studies have identified asteroids which could be injected into manifolds which wind onto periodic orbits around collinear Lagrangian points of the Sun-Earth system, by means of a low-cost manoeuvre. However, the periodic orbits as well as the manifolds are highly unstable, and small errors in the capture manoeuvre would bring to complete mission failure, with potential danger of collision with the Earth itself. The main source of injection error in position and velocity is the epistemic uncertainty of the asteroid mass, which cannot be measured directly. For this reason, asteroid orbit control will be a strict requirement for such mission. This paper investigates the controllability of some asteroids during the transfer and along the period orbits, assuming the use of a solar-electric low-thrust engine. The control scheme is based on a linear quadratic regulator. A stochastic simulation with a Monte Carlo approach is used to simulate a range of different perturbed initial conditions. Results show that only a small subset of the considered combinations of trajectories/asteroids are reliably controllable, and therefore controllability must be taken into account in the selection of potential targets.

I. INTRODUCTION

Recent studies have suggested that near-Earth asteroids (NEAs) could be harvested and exploited for resources[1]. It is in fact well known that some NEAs are potentially full of strategic resources for in-space utilization (e.g., future in-orbit construction of space components) or even precious metals that may find interest in terrestrial commodity markets[2]. Harvesting asteroids will without doubt be costly; however more and more space companies have shown interest in this idea, as the benefit might overcome the cost in a relatively near-term.

A scenario that seems, arguably, as directly borrowed from the sci-fi, that of a rendezvous with an asteroid, to lasso it and haul it back to Earth neighbourhood, was recently announced as a mission concept under serious consideration by NASA*. However, evidences on the interest of the concept can also be found in the preceding growth of scientific output on the concept[3-7].

A scenario which was investigated in the last few years consists of modifying the NEA's orbit such as to capture it into a libration orbit of the Sun-Earth system[8] – Halo, planar or vertical Lyapunov. The asteroid's motion may then remain indefinitely on a periodic orbit near a libration point, which is relatively accessible from Earth, or alternatively transferred to other regions of the cislunar space (e.g., Moon orbit[6]).

Recently, García et al.[8] identified asteroids which could be injected into manifolds which wind onto periodic orbits around collinear Lagrangian points of the Sun-Earth system, by means of two low-cost capture manoeuvres.

However, it is known that the considered periodic orbits as well as the associated manifolds are highly unstable, and small errors in the capture manoeuvre would bring to departure of the asteroid from the reference trajectory in a short time. The intrinsic risk of this scenario is the possibility to divert the asteroid's trajectory in a way that it could impact the Earth.

This paper therefore aims to provide a more accurate account of the towing manoeuvre required to place an asteroid on a libration point orbit near the Sun-Earth L_1 or L_2 points. The paper investigates the optimal control of the towing spacecraft during two distinct phases: firstly, at Earth approach, when the asteroid is still far but slowly approaching the Earth following a stable invariant manifold trajectory; secondly, after the insertion into a target libration orbit, as station keeping is still necessary in order to keep the asteroid from drifting away and causing any potential concern for the Earth. By means of a Monte-Carlo analysis, we quantify the control margins necessary to ensure that the asteroid does not divert irreparably on a different trajectory, and hence becomes a risk for the Earth. In addition, a range of potentially useful target orbits near the libration

* http://www.nasa.gov/sites/default/files/files/AsteroidRedirectMission_FS_508_2.pdf [retrieved 4 Sep 2013]

points are analysed in terms of station-keeping costs and safety.

In this paper, we will quantify the uncertainties of the state vector of the asteroid-spacecraft system, after the capture manoeuvres, due to epistemic uncertainty on the mass of the asteroid. Given these perturbed states, a feedback control based on a linear quadratic regulator will be used to pilot a low-thrust engine to bring the system on the reference trajectory towards the final periodic orbit. A Monte Carlo approach will be used to generate a variety of different initial perturbed states and obtain some statistical results on the controllability of each combination of asteroid and trajectory.

II. ASTEROID RETRIEVAL TRAJECTORIES

II.I. Equations of motion

For representing the trajectories in this paper, the equations of motion of the normalised circular restricted three-body problem[9] (CR3BP) in a Sun-Earth synodic reference frame are used:

$$\begin{aligned} \ddot{x} &= 2\dot{y} + \frac{\partial \Omega}{\partial x} + \frac{T_x}{m} \\ \ddot{y} &= -2\dot{x} + \frac{\partial \Omega}{\partial y} + \frac{T_y}{m} \\ \ddot{z} &= \frac{\partial \Omega}{\partial y} + \frac{T_z}{m} \end{aligned} \qquad [1]$$

with:

$$\Omega = \frac{x^2 + y^2}{2} + \frac{1-\mu}{r_S} + \frac{\mu}{r_E}$$

where r_S, r_E are the distances to the Sun and the Earth respectively and $\mu = 3.0032 \times 10^{-6}$ for the Sun-Earth system. **T** is the thrust vector, and m is the mass of the spacecraft and the asteroid, which are supposed to be tightly connected as a single point mass (Fig. 1).

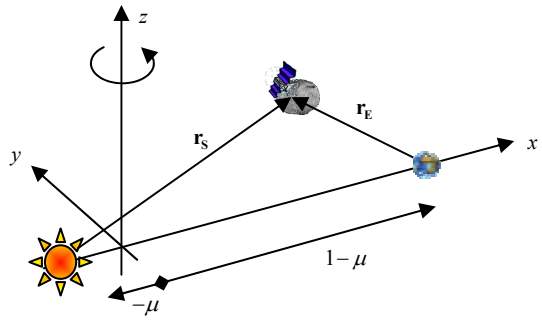

Fig. 1. Schematic of the CR3BP and its equilibrium points.

As is well known, when the thrust vector is zero, the system in Eqs. [1] has five equilibrium positions (see Fig. 2). The Sun-Earth L_1 and L_2 points are of particular interest for us, since they are the *gate keepers* for potential ballistic capture of asteroids in the Earth's vicinity.

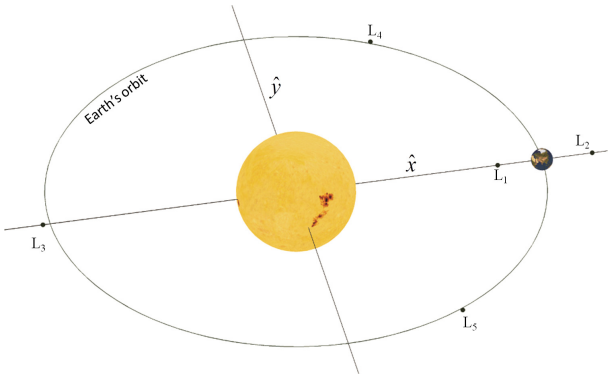

Fig. 2. Schematic of the CR3BP and its equilibrium points.

The phase space near these equilibrium regions in the CR3BP can be divided into four broad classes of motion: bound motion near the equilibrium position, asymptotic trajectories that approach or depart from the latter, transit trajectories, and non-transit trajectories (see Fig. 3 for this division).

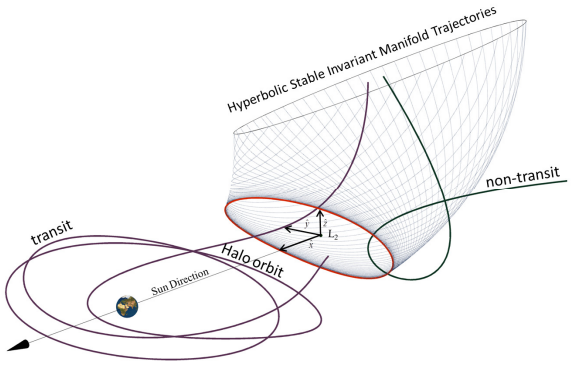

Fig. 3. Schematic representation of the four categories of motion near the L_2 point (represented by the set of axes in the figure): periodic motion around L_2 (i.e., halo orbit), hyperbolic invariant manifold structure (i.e., set of stable hyperbolic invariant manifold trajectories), transit trajectory and non-transit trajectory.

II.II. Retrieval trajectories

Motivated by the recent interest on asteroids, and most particularly on the most accessible subset of its population, García et al.[8] carried out an exhaustive search for asteroids whose unperturbed trajectories laid close to an stable invariant manifold trajectories leading to one of the following distinct classes of periodic motion near the Sun-Earth L_1 and L_2 points: Planar (P),

Vertical (V) Lyapunov and Halo Orbits north (Hn) and south (Hs).

Each of these families of libration point orbits (LPOs) is in fact a continuous set of periodic motion that can be explored by means of numerical continuation process with increasing Jacobi Constant (i.e., energy). Fig. 4 shows a discretised set of Planar and Vertical Lyapunov orbits that cover Jacobi constants ranging from 3.0007982727 to 3.0000030032. Ticker red line corresponds to a Jacobi constant of 3.0004448196, which corresponds to half distance between the energy at equilibrium in L_2 and L_3.

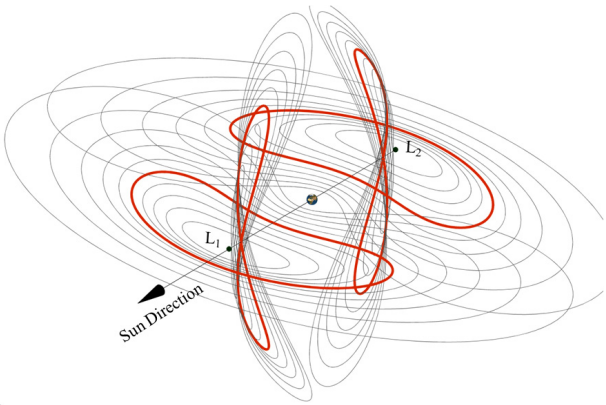

Fig. 4. Series of Planar and Vertical Lyapunov orbits associated with the Sun-Earth L_1 and L_2 points.

From each of these LPOs, a hyperbolic invariant stable manifold can be generated that consist of an infinite number of trajectories exponentially approaching the periodic orbit to which they are associated. A subset of invariant stable manifold trajectories, such as the one represented in Fig. 3, can be propagated backwards in the CR3BP framework for an arbitrary time.

In García et al.[8] these trajectories were propagated to a planar section located at a $\pi/8$ angle with the Sun-Earth line. This section corresponds roughly to a distance to Earth of the order of 0.4 AU, where the gravitational influence of the planet is considered small. Hence, from this section outwards, these trajectories could be well approximated in two-body motion, and thus described analytically by means of constant orbital elements. Note that the only exception the longitude of the perihelion, i.e., the sum of the right ascension of the ascending node and the argument of perihelion, which varies with a simple function of time due to the motion of the Earth on its orbit[8].

Finally, as depicted in Fig. 5, the sets of orbital elements associated with stable invariant manifold trajectories at the $\pi/8$ section form the basis for a *bulleye* orbit targeting that was solved as an heliocentric Lambert arc of a restricted two-body problem with two impulsive burns, one to depart from the NEO, the final one for insertion into the manifold, with the insertion constrained to take place before or at the $\pm\pi/8$ section. These capture transfers can then be defined with 5 variables: the Lambert arc transfer time, the manifold transfer time, the insertion date at the target periodic orbit, the energy of the final orbit, and a fifth parameter determining the point in the target orbit where the insertion takes place. The optimal transfer opportunities where then found by a global search that uses a stochastic search blended with an automatic solution space decomposition technique[10]. Table 1 summarises the best trajectories found in Ref. [10] for each type of target orbit for L_2 and L_1.

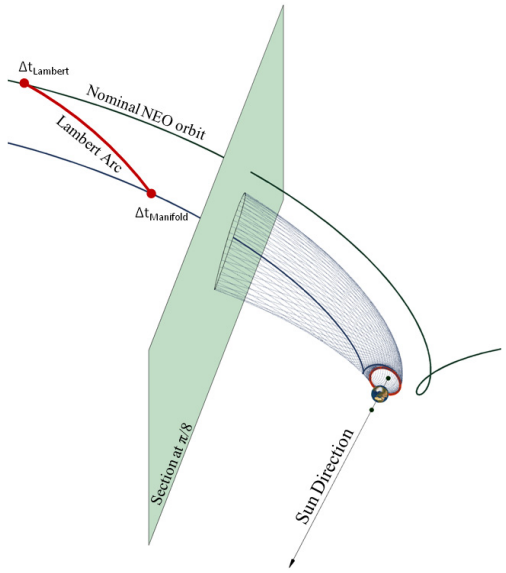

Fig. 5. Schematic representation of a transfer to L_2.

Despite the fact that the work presented in Ref. [10] also discusses the possibility that these trajectories could be flown, the conclusions were based solely on the transfer costs involved and the capability of current propulsion systems to provide the necessary change of linear momentum. This work, on the other hand, will deal with another critical issue with regards the feasibility of these trajectories; the controllability of the asteroid during the towing and parking process, in particular to avoid any unnecessary collisional risk with Earth or other human asset in space. Hence, the paper will attempts to provide further considerations on the feasibility of these trajectories by focusing on the 8 transfers described in Table 1, which cover all types of periodic motion considered in García et al.[10]

	Asteroid name	Orbit destination	Date [yyyy/mm/dd]			Energy of Manifold	Total Duration [yrs]	Δv [m/s]		
			Asteroid departure	Manifold insertion	L_1 or $L_{1/2}$ arrival			Dep	Ins	Total
1.	2011 UD21	1Hn	2037/11/20	2038/07/03	2042/07/19	3.000411	4.66	149	207	356
2.	2011 UD21	1Hs	2039/10/24	2040/06/15	2043/08/30	3.000504	3.85	210	226	436
3.	2000 SG344	1P	2024/02/11	2025/03/11	2027/06/18	3.000357	3.35	195	248	443
4.	2011 UD21	1V	2036/07/20	2038/11/16	2041/06/21	3.000667	4.92	226	196	422
5.	2006 RH120	2Hn	2021/02/01	2024/03/30	2028/08/05	3.000421	7.51	58	0	58
6.	2006 RH120	2Hs	2023/05/11	2024/02/20	2028/08/31	3.000548	5.31	52	55	107
7.	2007 UN12	2P	2013/10/22	2016/04/28	2021/02/19	3.000069	7.33	199	0	199
8.	2010 VQ98	2V	2035/02/14	2035/09/01	2039/11/15	3.000016	4.75	177	4	181

Table 1. Asteroid reference trajectories.

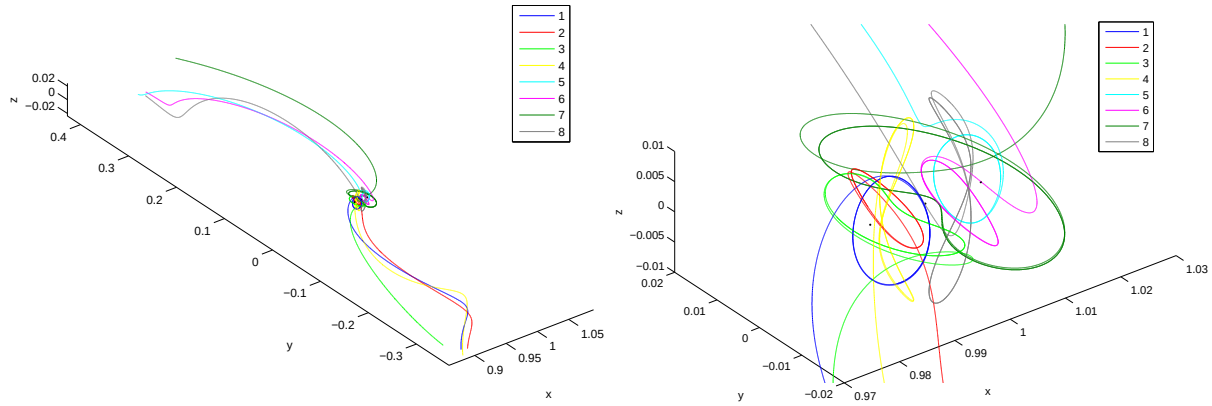

Fig. 6. Asteroid trajectories to periodic orbits considered.

Fig. 6 depicts these 8 capture trajectories. Two distinct parts compose these trajectories: the hyperbolic stable invariant manifold trajectory that approaches the equilibrium point and the periodic motion near the equilibrium point. These two parts are entirely ballistic trajectories, which, in the original work[10], were assumed to be flown with negligible correction manoeuvres. The 8 trajectories include also one complete period along their respective periodic orbit. It is here assumed that if it is possible to control the asteroid-spacecraft in the final part of the transfer and for one period of the periodic orbit, then further periods could also be controlled. All these trajectories will be used as reference in the following, for the feedback control algorithm.

II.III. Uncertainty estimates for the manifold insertion

The trajectories in the previous section were computed assuming ideal conditions, i.e. all variables in the problem were exactly known. However, there are a number of uncertainties affecting the problem, the most important of which being the asteroid mass. In this work, we assume that the epistemic uncertainty on the mass of the asteroid to haul introduces an error on the velocity at the manifold insertion. While it is true that many other sources of error should be expected, such as inaccuracies on the thrust direction and magnitude, it is believed, as will be discussed below, that the single major source of uncertainty will be due to inaccuracies on the inertial mass of the object.

Itokawa's mass measurements it is a good example of this issue[11]. Hayabusa spacecraft visited asteroid Itokawa during late 2005. An estimate of its mass was calculated to an accuracy of 3% by means of several different measurements of tracking and navigation data during different intervals. However, an asteroid retrieval mission will be expected a higher accuracy than that, since on addition to the remote measurements, a retrieval mission will be able to perform a series of initial pushing manoeuvres to calibrate the system once the asteroid has been safely attached to the spacecraft. These initial manoeuvres should increase considerably the accuracy of the mass of the system.

In this paper, nevertheless, we assume in 1% the epistemic error of the mass of target asteroid, after all measurement phase is completed, and thus, we study if such a mission could recover from that error at the insertion of the manifold trajectory.

Note however that we should distinguish between the residual epistemic uncertainty on the asteroid's mass by the time the asteroid retrieval phase is carried out and the lack of information available today on the asteroids in Table 1. The former is assumed to affect the reliability of a mission attempting to move an asteroid of a roughly known mass. The latter is only an added difficulty when attempting to make this analysis

relevant to the asteroids in Table 1. In the fictitious scenario of an attempt to retrieve the asteroids in Table 1, a possible sequence of Earth remote observations, if opportunity arise, possible precursor missions, approaching phase of the retrieval spacecraft and final pushing manoeuvres to calibrate the system should reduce the uncertainty of the mass of the asteroid to 1%.

Yet, the mass of the asteroid in Table 1 is today unknown, as happens with most of the asteroids, except for those that have been visited by a spacecraft or have a small companion orbiting it (i.e., binaries). Thus, it must be inferred from the only available information on the asteroid's physical characteristics: the absolute magnitude H. The mass can then be estimated as[12]:

$$m_{ast} = \frac{\pi}{6}\rho\left(\frac{1.329\cdot 10^6}{\sqrt{p_v}}10^{-H/5}\left[\mathrm{m}\right]\right)^3 \qquad [2]$$

where ρ is the asteroid's density and p_v the albedo. Both ρ and p_v need to be assumed and average values for these two parameters are generally used[13]. Hence, due to plausible deviation from the average value of ρ and p_v, Eq. [2] provides only a rough estimate of the asteroid's mass that can easily be wrong by half an order of magnitude. Hence, as suggested in Ref. [13], this paper uses a mean value for $\rho\left(p_v\right)^{-3/2}$ based on the standard NEA (i.e., 43,000 kg/m^3) and minimum and maximum based on S-class asteroids (i.e., 35,000 kg/m^3) and M-class asteroids (i.e., 127,000 kg/m^3) respectively. Therefore, for each asteroid in Table 1, three possible masses were considered, which take into account the mean, minimum and maximum possible values.

Mass inaccuracies error propagation

If a particular asteroid transfer is expected to require a given change in velocity Δv_{tran}, we thus need to supply our system with a total change of linear momentum:

$$I_{tran} = \left(m_{ast} + m_{s/c}\right)\cdot \Delta v_{tran} \qquad [3]$$

Or, by assuming I_{tran} as a requirement to follow the trajectory, we can rewrite:

$$\Delta v_{tran} = \frac{I_{tran}}{m_{ast} + m_{s/c}}$$

By considering a small error on the asteroid mass δm_{ast}, and taking the difference of the previous equation, it is possible to relate it to the error in velocity change:

$$\delta\Delta v_{tran} = \frac{I_{tran}}{\left(m_{ast} + m_{s/c}\right)^2}\delta m_{ast}$$

Which, by substituting I_{tran} as in Eq. [3] and assuming that $m_{s/c}$ is negligible when compared with the mass of the asteroid m_{ast}, can be rewritten as:

$$\delta\Delta v_{tran} \approx \Delta v_{tran}\frac{\delta m_{ast}}{m_{ast}}$$

Hence if 1% is the relative epistemic error of the mass of target asteroid, 1% is also the uncertainty in velocity. This 1%, however, is the uncertainty generated right after an impulsive manoeuvre. This error need to be propagated for the length of the transfer to account for the actual position and velocity uncertainty at the manifold insertion.

Definition of the perturbed initial states

In a dynamical system such as the CR3BP, the difference between two neighbouring trajectories with initial states:

$$\bar{\mathbf{s}}\left(0\right) = \mathbf{s}_0$$
$$\mathbf{s}\left(0\right) = \mathbf{s}_0 + \delta\mathbf{s}_0$$

can be efficiently propagated by means of an error state transition matrix, such as:

$$\delta\mathbf{s} = \mathbf{\Phi}\left(t, t_0\right)\delta\mathbf{s}_0$$

where the state transition matrix $\mathbf{\Phi}\left(t, t_0\right)$ is numerically integrated as:

$$\dot{\mathbf{\Phi}}\left(t, t_0\right) = \mathbf{A}\left(t\right)\mathbf{\Phi}\left(t, t_0\right)$$
$$\mathbf{\Phi}\left(t_0, t_0\right) = \mathbf{I}$$

and $\mathbf{A}\left(t\right)$ is the matrix of partial derivatives of the system, or Jacobian matrix[14].

This procedure allows computing, at the time of the manifold insertion, the error in the states as a consequence of the capture trajectory. The errors in Table 2 were found, for each trajectory. These errors will be used as initial state errors for the following integration.

Table 2. Errors $\delta\mathbf{s}$ on initial state vector.

	Position			Velocity		
	km	km	km	km/s	km/s	km/s
1	258600.1	108470.5	9775.522	0.024072	0.054863	0.001739
2	565034	202118.9	5523.523	0.043882	0.118125	0.003175
3	98750.57	316358.6	3576.452	0.059853	0.011538	0.000654
4	366629.4	135921	2841.328	0.028196	0.077596	0.001455
5	52195.46	147807.4	2116.254	0.029871	0.007961	0.000661
6	147585.2	221997.3	1204.072	0.041671	0.030086	0.000614
7	145383.5	704180.8	3144.984	0.120402	0.02459	0.001125
8	293976	86877.72	7883.155	0.012487	0.060326	0.001102

As mentioned previously, the error on the mass of the asteroid-spacecraft system, is taken as 1% of the mass of the reference mass of asteroid.

The errors in Table 2 are used to generate the random initial states for the feedback control algorithm (see Fig. 7). A random normal distribution of points is generated, using the ellipsoid of uncertainty δs_i in Table 2 as 3σ:

$$s_i = s_{r,i} + \delta s_i \frac{\text{rndNorm}}{1.96} k \qquad [4]$$

The index i refers to each one of the states, rndNorm is a randomly generated number following a normal distribution with zero mean and unitary standard deviation, and finally k is a safety margin. The 1.96 normalisation guarantees that the sample points are inside the ellipsoid of uncertainty, times the safety margin, with 97.5 % probability.

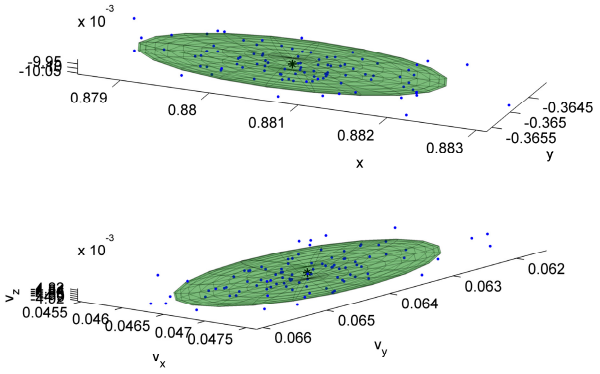

Fig. 7. Ellipsoids of uncertainty for position and velocity, and randomly sampled points for trajectory 1.

III. MONTE CARLO APPROACH

A Monte Carlo method is used to assess the control of the asteroids on their respective trajectories, for a number of random initial conditions.

The reference state is perturbed at the π/8 section in Fig. 5 (i.e. the beginning of the trajectories in Fig. 6a), where the controlled phase begins. This perturbation is modelling a different state in which the asteroid-spacecraft system might be, after the capture manoeuvres, due to the uncertainty on the mass of the asteroid, as well as imperfections in the Δv delivery from the thruster.

One hundred random points are generated using Eq. [4] for each trajectory. In addition, for each trajectory, two different values of the safety margin are used: $k = 1$ and $k = 10$.

Fig. 8 shows a brief pseudo-code of the algorithm used to generate the sample points and run the control simulation on each one of them.

```
For trajectory = 1, …, 8
  For mass = min, mean, max
    For k = 1, 10
      For point = 1…100
        Generate random initial state
        Run control simulation
        Check success
      End
    End
  End
End
```

Fig. 8. Pseudo-code for the Monte Carlo simulation.

Once each perturbed initial state is generated, the feedback control simulation is run, to assess whether it is possible to recover the spacecraft onto the reference trajectory.

IV. CONTROL SCHEME

Each perturbed initial state is propagated adding a feedback control with the aim to restore the reference conditions. The control loop used here is based on a linear quadratic regulator (LQR)[15], applied in a similar way as in Ceriotti et al.[16]

As actuator for the control loop, we assume to have a solar electric propulsion (SEP) thruster, whose characteristics are similar to the one considered by the NASA asteroid retrieval mission study[6]. In particular, the power available is $P_{SEP,max} = 40$ kW (here considered constant, not varying with the distance of the

Sun) and the specific impulse is $I_{sp} = 3000$ s, from which the maximum thrust can be computed as:

$$T_{max} = 2P_{SEP,max}\eta_{SEP} / I_{sp} g_0 = 1.9 \text{ N} \quad [5]$$

where $\eta_{SEP} = 0.7$ is the efficiency of the SEP system[17] and $g_0 = 9.81$ m/s^2 is the standard gravity acceleration.

The actual thrust that the thruster can deliver is continuously adaptable between 0 and T_{max} at any given time. It is also assumed that the thrust direction is not constrained, in the sense that the spacecraft (attached to the asteroid) has an attitude control system that is able to re-orient the nozzle in the direction of the required thrust. A control vector can therefore be defined as:

$$\mathbf{u} = \begin{bmatrix} T_x & T_y & T_z \end{bmatrix}^T$$

subject to the non-linear constraint $\|\mathbf{u}\| < T_{max}$.

For defining the control strategy, it is convenient to rewrite the equations of motion [1] as a first-order differential system $\dot{\mathbf{s}} = \mathbf{f}(t, \mathbf{s})$, including the mass, introducing the state vector $\dot{\mathbf{s}} = \begin{bmatrix} x & y & z & v_x & v_y & v_z & m \end{bmatrix}$, where $\mathbf{v} = \dot{\mathbf{r}}$ and the dynamical equation of the mass change is:

$$\dot{m} = -T / I_{sp} g_0$$

Let us assume, at a given instant of time $\bar{t}$, that the spacecraft is at state $\mathbf{s}(\bar{t})$. At the same time, the reference state is $\mathbf{s}_r$ and the reference control is null, as the nominal trajectory is purely ballistic. The reference state defines the reference orbit as function of time, as discussed in the previous section. In an ideal condition, the real state coincides with the reference one. However, due to the instability of the trajectory and the uncertainty in the initial conditions, in general the real state may differ from the reference one, and therefore the state error can be defined as: $\delta\mathbf{s} = \mathbf{s} - \mathbf{s}_r$. The objective of the controller is to find the control $\mathbf{u}$ (defined as the feedback control) that brings the spacecraft states back to the reference states after some time.

To compute **u** at each instant of time, we use here a linear time-invariant approximation of the dynamical system. Due to this approximation, the real state shall be in the vicinity of the reference state. Furthermore, if we assume that the dynamics of the reference trajectory is slow enough, then we can approximate the time varying problem as a sequence of time-invariant problems, and use classic linear feedback control theory for computing the gain matrix. The optimal control problem is solved at each instant of time, and the gain matrix updated, as described in the following. It is not to be required to follow the mass state within the control: hence, the linearisation is done in the following way:

$$\mathbf{A}_{6\times6} = \left.\frac{\partial \mathbf{f}}{\partial \mathbf{s}}\right|_{\mathbf{s}_r} \; ; \; \mathbf{B}_{6\times3} = \left.\frac{\partial \mathbf{f}}{\partial \mathbf{u}}\right|_{\mathbf{s}_r}$$

The derivatives of **f** with respect to states (except the mass) **A** and controls **B** are found analytically (their expression is omitted here), and then evaluated numerically. The dynamics of the system in the vicinity of $\mathbf{s}_r$ can then be expressed as:

$$\delta\dot{\mathbf{s}} = \mathbf{A}\delta\mathbf{s} + \mathbf{B}\mathbf{u} \quad [6]$$

This linear, time-invariant system approximates the real system at a given time and in the vicinity of the reference states. It can be verified through the controllability matrix that the system in Eq. [6] is controllable. However, non-linearities, as well as the saturation of the thrust, will limit the applicability of this method to some maximum displacement from the reference. The problem is now to find the optimal feedback control history $\mathbf{u}(t)$ for any time $t > \bar{t}$ such that the (linear) system of Eq. [6] will settle to the reference state, i.e. $\delta\mathbf{s} = 0$. We introduce the following cost function:

$$J(\mathbf{u}) = \int_0^\infty \left(\delta\mathbf{s}^T\mathbf{Q}\delta\mathbf{s} + \mathbf{u}^T\mathbf{R}\mathbf{u}\right)dt \quad [7]$$

which aims at minimising the state error and the feedback control over an infinite amount of time, constrained to the linear system in Eq. [6]. The matrices **Q** and **R** are weights that quantify the relative cost of each state and control in the cost function.

We now assume a control proportional to the state error, $\mathbf{u} = -\mathbf{K}\delta\mathbf{s}$. Minimizing Eq. [7] under this assumption leads to the well-known algebraic Riccati equation [15], which can be solved analytically to compute the gain matrix $\mathbf{K}_{3\times6}$.

The total control can then be computed, and saturation is applied according to the maximum thrust values presented in Eq. [5]. The resulting thrust is then fed into the integration of the full equations of motion, including the mass flow. At the next time step in the integration, the procedure is restarted to update the feedback control: the gain matrix is computed dynamically during the simulation.

For this problem, considering the normalisation of the variables introduced in the CR3BP, the following weights were used:

$$\mathbf{Q} = \text{diag}\left(\begin{bmatrix} 10^6 & 10^6 & 10^6 & 10^3 & 10^3 & 10^3 \end{bmatrix}\right)$$

$$\mathbf{R} = \text{diag}\left(\begin{bmatrix} 10^{36} & 10^{36} & 10^{36} \end{bmatrix}\right)$$

The choice of these coefficients was done initially following Bryson's rule ($\mathbf{Q}, \mathbf{R}$ diagonal with Q_{ii} = maximum acceptable value of δs_i^2, R_{ii} = maximum acceptable value of u_i^2), and then adjusted with a heuristic procedure. Note that the large values of **R** are

essentially a scaling factor due to the thrust being expressed in non-dimensional units of the CR3BP.

IV.I. Application to asteroid control

The control simulation runs for a time equivalent to the time it takes for the reference trajectory to wind onto the periodic orbit and complete one period on it. After this time, the states of the simulation are compared with the states of the reference trajectory: if their distance is small (1e-4 in position and 1e-3 in velocity), then the control is considered successful. Note that it was experienced that these tolerances are not affecting the results, in the sense that if the control is successful, then it very easily acquires the reference well below these tolerances; vice-versa, when the control is not sufficient, then the spacecraft diverges completely, causing a final separation from the reference that is of orders of magnitude greater than the tolerances.

Fig. 9 shows two controlled trajectories, starting from two different random points based on the same reference trajectory (namely trajectory 1, mass 419,799 kg, $k = 1$): on one of them the control is successful, and in fact it is extremely close to the reference; the other trajectory, instead, diverges. The spacecraft does not get close to the reference for the whole manifold, for then departing considerably once on the periodic orbit.

For the successfully controlled solution, Fig. 10 shows the state error, i.e. the difference between the real state and the reference state, in terms of position and velocity. The same figure also shows the mass flow (considering 0 the initial mass at the beginning of the controlled phase). This gives an estimation of the propellant mass required for the control of the asteroid during the transfer and one period around the orbit. Fig. 11 shows the required thrust in Cartesian components and magnitude. The trend is typical of an LQR controller, with a high amount of thrust at the beginning, to reduce the initial state error, and then some residual thrust to counterbalance the instabilities of the system.

In these plots, time is in the CR3BP conventional non-dimensional units, i.e. 1 year corresponds to 2π, and $t = 0$ corresponds to the insertion into the periodic orbit.

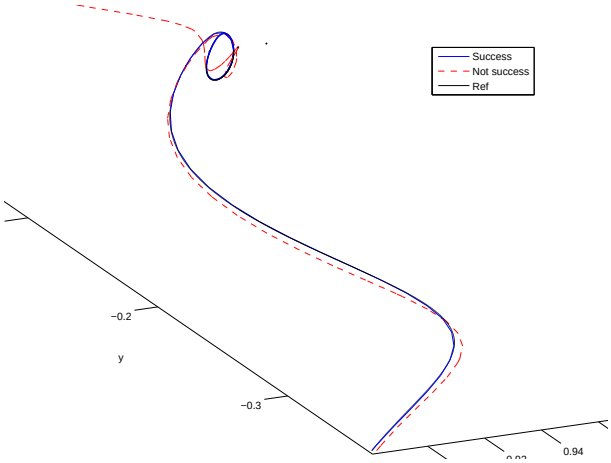

Fig. 9. Two random initial states on trajectory 1 that lead to successful or unsuccessful control.

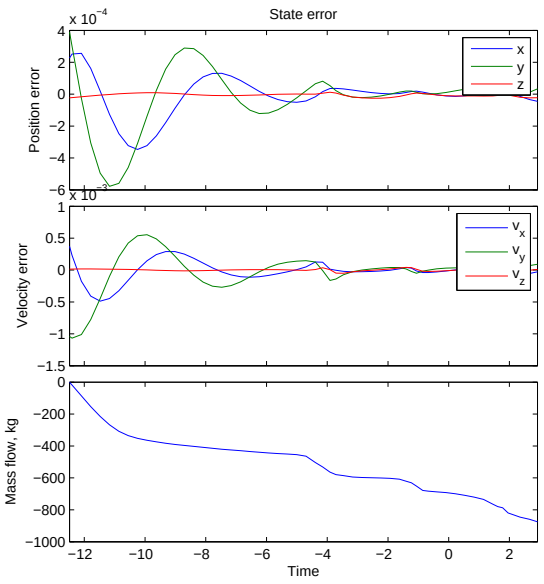

Fig. 10. State error with respect to reference (position, velocity) and mass flow.

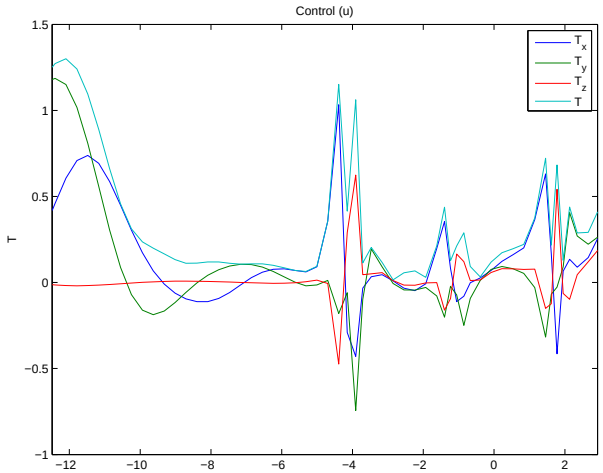

Fig. 11. Control thrust.

V. RESULTS

The success rate for each trajectory, value of nominal mass and safety margin is collected and shown in form of histograms in the following Fig. 12, showing the rate of success over the hundred simulations. Each plot refers to a trajectory, and contains three (double) columns, each one referring to minimum, mean and maximum mass of the asteroid on that trajectory. Finally, within each column, each histogram bar refers to the two values of the safety margin.

The first thing to note is that, because the thrust level is limited, the success rate is heavily affected by the mass of the asteroid. The acceleration that the thruster can provide is in fact inversely proportional to the mass of the system. For example, trajectory 3 is associated with a trajectory to retrieve asteroid 2000SG344, with a derived size ranging from 20 to 70 meters diameter. This object is by far the largest object that is considered for retrieval and, it is evident from Fig. 12, that the object would not be controllable with the assumed thrusting capability.

However, trajectory 1, 2 and 4 are associated with the same asteroid, 2011 UD21, and hence the spacecraft is carrying the same mass. Yet, the success rate of trajectory 4 is much higher than that of 1 and 2. It is therefore apparent that the asteroid's controllability does not solely depend on the mass of the object to be towed, but in many other factors, such as the type of LPO and energy that is targeted, the Δv of each manoeuvre, the lengths of the coasting arcs, etc. All this factors affect the controllability of these trajectories in conjunction, and is thus difficult to isolate their particular effects.

This dependence to many intertwined factors is evident, for example, in trajectories 5 and 6, which are associated with the smallest asteroid of the set, and indeed they have the highest success rates. Both of these trajectories target a Halo orbit, albeit one to the southern family and the other to the northern one. The stability of both families is expected to be similar, and, as expected, both success rates are similar. However, it is noticeable that for trajectory 6 the success rate decreases when considering the maximum mass, which does not happen for trajectory 5, for which the success rate is always 100% regardless of the mass case; it decreases only when considering the additional safety margin $k = 10$.

In order to uncouple the effect of the asteroid's mass on the response of the feedback control performance for a given trajectory, another set of Monte Carlo simulations was run: this time, the same values of mass were used for all the trajectories: 100,000 kg, 500,000 kg and 1,000,000 kg. The results for this set of simulations are presented in Fig. 13, in the same format as before.

This second simulation allows us to see that, for example, trajectory 3 has a 100% success rate on the lowest mass estimate, higher than in trajectories 1, 2, 4 and 6. We can therefore conclude that the controllability of trajectory 3 itself is in fact higher than others, however the huge mass of the asteroid 2000SG344 associated to this trajectory makes it unfeasible, as discussed previously.

It is also noteworthy, for masses >100,000 kg, that trajectory 8 is more controllable than trajectory 6, despite the fact that trajectory 8 targets a much larger energy (i.e., lower Jacobi constant) LPO than trajectory 6 does.

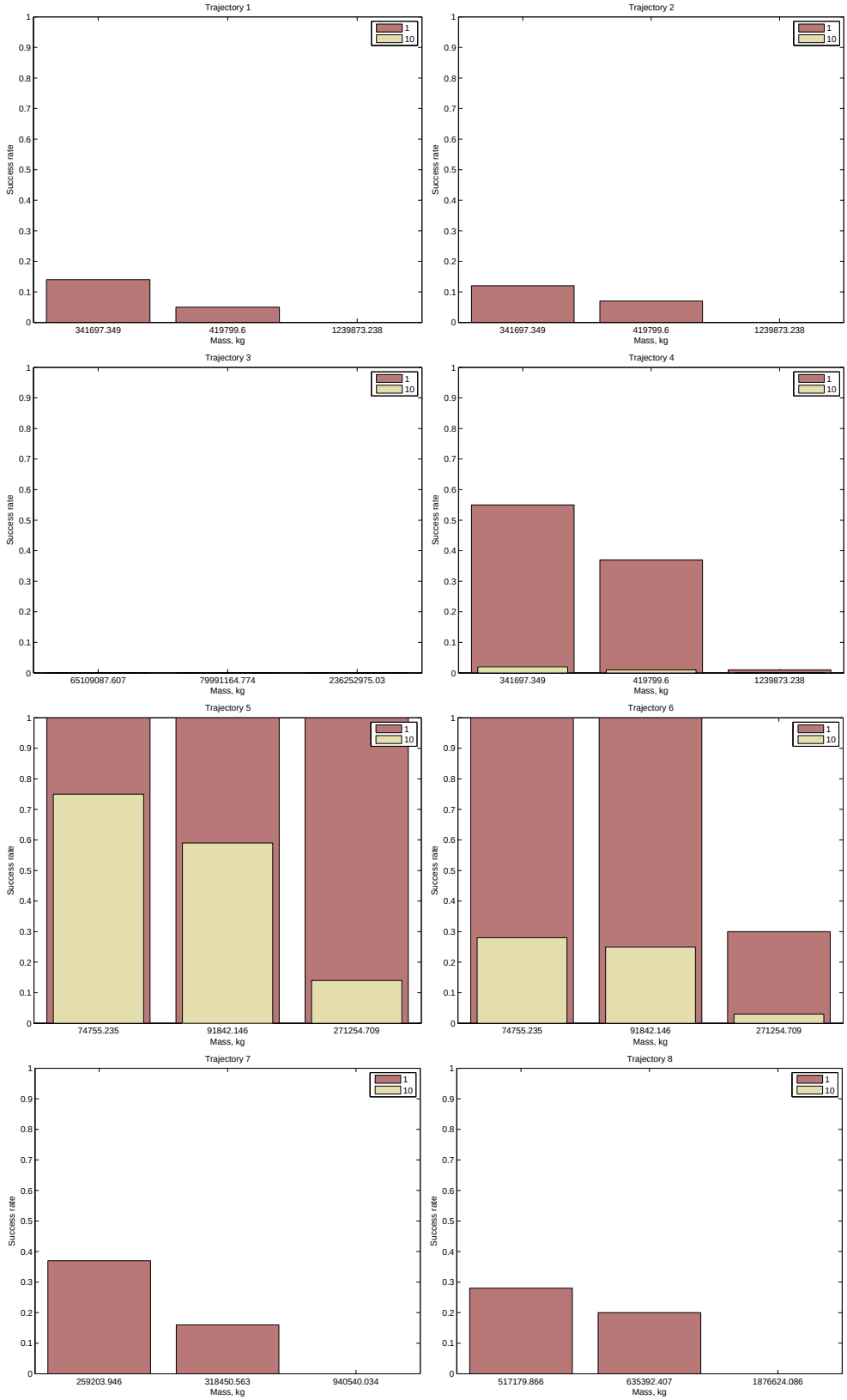

Fig. 12. Statistical results of Monte Carlo simulation of the control. Each plot refers to one trajectory, and it includes the success rate for three different asteroid masses and two values of the safety coefficient.

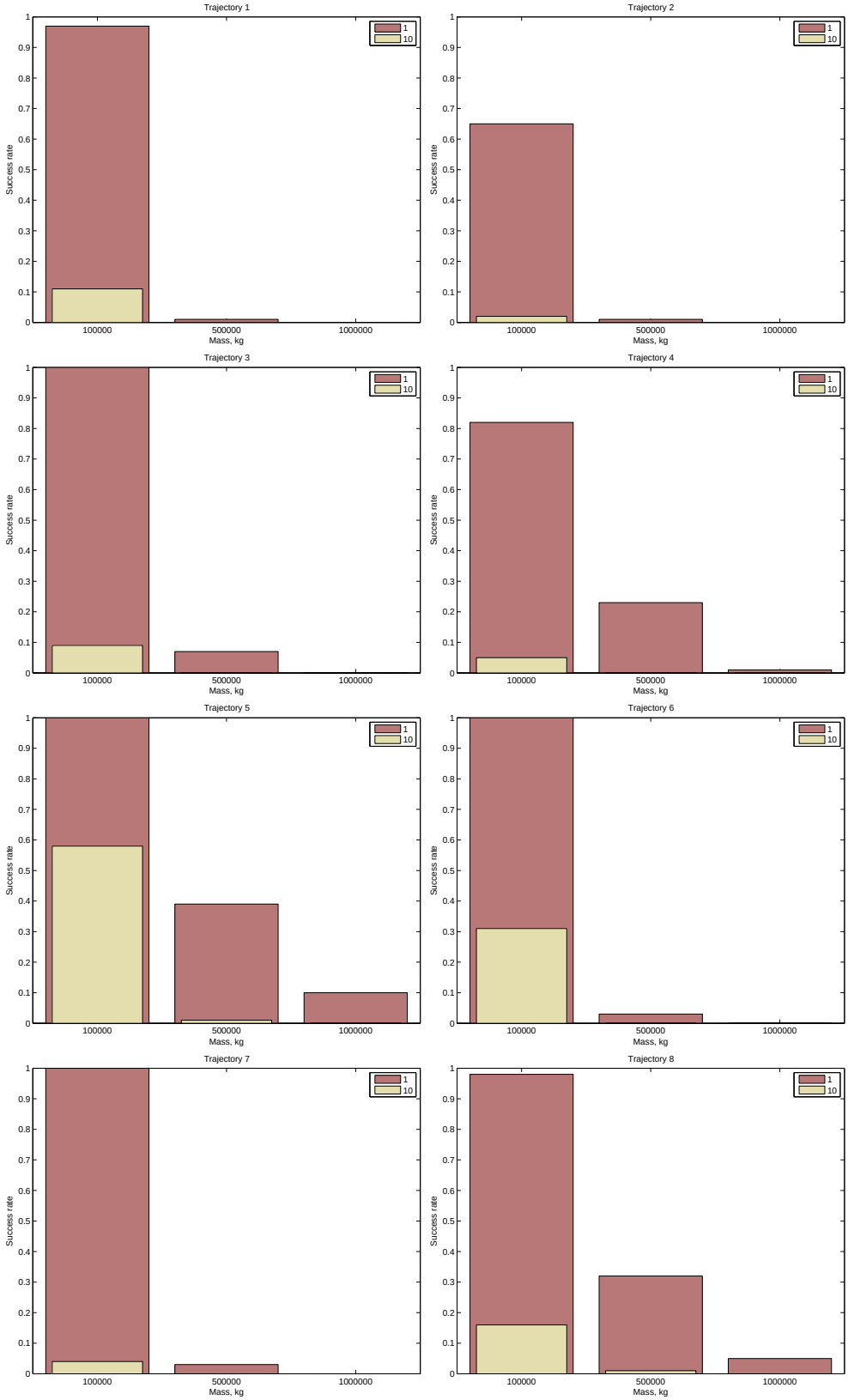

Fig. 13. Statistical results of Monte Carlo simulation of the control, using the same mass values for all the trajectories.

VI. CONCLUSIONS

The control of the asteroid along its trajectory to the periodic orbit, and along the periodic orbit itself, is a serious issue. It resulted that some of the combinations of trajectories/asteroids simply cannot be controlled with the proposed propulsion technology. Vice-versa, the Monte Carlo simulation showed that some other combinations are very robust, and the asteroid can be controlled even in case of large errors in the deflecting Δv. Given the hazard that an uncontrolled NEO can pose to the Earth, this paper has shown that the controllability of the system should therefore be one of the key parameters to be taken into account for the choice of the candidate asteroids to be hauled.

ACKNOWLEDGEMENTS

J.P. Sanchez would like to acknowledge the support of the European Commission under the Marie Curie grant 330649 (AsteroidRetrieval).

[1] V. E. Badescu, "Asteroids - Prospective Energy and Material Resources", ed. V.E. Badescu, Springer, 2013
[2] J. S. Lewis, "Mining the sky: untold riches from asteroids, comets and planets", Helix Books/Perseus Books Reading, Massachusetts, 1996
[3] H.-X. Baoyin, Y. Chen, J.-F. Li, "Capturing near earth objects", *Research in Astronomy and Astrophysics*, vol. 10, n. 6, p. 587-598, 2010
[4] J. P. Sanchez, C. R. McInnes, "Asteroid Resource Map for Near-Earth Space", *Journal of Spacecraft and Rockets*, vol. 48, n. 1, p. 153-165, 2011
[5] Z. Hasnain, C. Lamb, S. D. Ross, "Capturing near-Earth asteroids around Earth", *Acta Astronautica*, vol. 81, n. 2, p. 523–531, 2012
[6] J. Brophy, et.al, "Asteroid Retrieval Feasibility Study", Keck Institute for Space Studies, Califonia Institute of Technology, Jet Propulsion Laboratory, Pasadena, California, 2012
[7] N. Lladó, J. Masdemont, G. Gomez, Y. Ren, "Capturing Small Asteroids into the Sun-Earth Lagrangian L1,L2 Points for Mining purposes", in *Proceedings of 63rd International Astronautical Congress 2012*, Naples, Italy, 2012
[8] D. García Yárnoz, J. P. Sanchez Cuartielles, C. R. McInnes, "Easily retrievable objects among the NEO population", *Celestial Mechanics and Dynamical Astronomy*, vol. 116, n. 4, p. 367-388, 2013
[9] R. H. Battin, "An introduction to the mathematics and methods of astrodynamics", Revised edition, *AIAA Education Series*, AIAA, New York, 1999
[10] M. Vasile, M. Locatelli, "A hybrid multiagent approach for global trajectory optimization", *J. of Global Optimization*, vol. 44, n. 4, p. 461-479, 2009
[11] A. Fujiwara, J. Kawaguchi, D. K. Yeomans, M. Abe, T. Mukai, et al., "The Rubble-Pile Asteroid Itokawa as Observed by Hayabusa", *Science*, vol. 312, p. 1330-1334, 2006
[12] E. Bowell, B. Hapke, D. Domingue, K. Lumme, J. Peltoniemi, et al., "Application of photometric models to asteroids", in *Asteroids II*, R.P. Binzel, R.P. Gehrels, and M.S. Matthews, Editors. 1989, Univ. of Arizona Press: Tucson. p. 524–556
[13] S. R. Chesley, P. W. Chodas, A. Milani, D. K. Yeomans, "Quantifying the Risk Posed by Potential Earth Impacts", *Icarus*, vol. 159, n. 2, p. 423-432, 2002
[14] D. A. Vallado, "Fundamentals of Astrodynamics and Applications", 3rd Edition, *The Space Technology Library*, ed. J.R. Wertz, Microcosm Press/Kluwer Academic Publishers, El Segundo, California, 2007
[15] A. E. Bryson, Y.-C. Ho, "Applied optimal control: optimization, estimation, and control (Revised printing)", Taylor & Francis Group, New York, 1975
[16] M. Ceriotti, C. R. McInnes, "Hybrid solar sail and solar electric propulsion for novel Earth observation missions", *Acta Astronautica*, vol. 69, n. 9-10, p. 809–821, 2011
[17] S. Kitamura, Y. Ohkawa, Y. Hayakawa, H. Yoshida, K. Miyazaki, "Overview and research status of the JAXA 150-mN ion engine", *Acta Astronautica*, vol. 61, n. 1-6, p. 360-366, 2007